

## A detailed examination on natural chromite as a heterogeneous catalyst in sono-Fenton process for removal of a cationic dye: Characterization and utilization potential

Özkan Açışlı\*, İlker Acar\*, Ercan Doğan

Department of Petroleum and Natural Gas Engineering, Faculty of Earth Sciences, Ataturk University, 25400, Oltu, Erzurum, Turkey, emails: ozkan.acisli@atauni.edu.tr (Ö. Açışlı), ilker.acar@atauni.edu.tr (İ. Acar)

Received 14 February 2019; Accepted 8 February 2020

### ABSTRACT

In this study, a chromite sample was examined as a heterogeneous catalyst in the ultrasound-assisted Fenton process for the removal of Malachite Green (MG) from aqueous solutions. Within this scope, the effects of operational parameters, scavengers, and various treatment processes on the removal efficiency of MG were studied as a function of retention time. In addition, the leachability characteristics of the chromite catalyst and intermediates produced during the degradation of MG were determined. The experimental results indicated that, for the equilibrium reaction time of 90 min, the efficiency of 88.73% was achieved with the chromite dosage of 3.0 g/L. However, the higher dosages resulted in a reduction, down to 61.61% for 5.0 g/L. Similarly, the efficiency values of 88.74% and 70.53% were obtained for the respective peroxide concentrations of 30 and 50 mM. On the other hand, the efficiency decreased gradually from 88.74% to 54.46% for initial MG concentrations of 10 and 100 mg/L, respectively. For 100 mg/L, the efficiencies of 30.31%, 64.03%, and 86.57% were obtained for the respective pH values of 3, 9, and 11. The combined effect of ultrasound and peroxide on the catalyst surface assured the optimum efficiency. Ethanol exhibited a more adverse effect than sodium chloride, where the efficiency reduced dramatically down to 38.22%. In addition, only 22.20% reduction was observed in the efficiency after four consecutive cycles. According to the leaching analysis, all of the examined metals have leaching capacities far below the toxicity levels for non-hazardous waste. GC-MS analysis confirmed the efficient degradation of MG during the process. Overall results have shown that the chromite sample provided promising results as a heterogeneous catalyst in a sono-Fenton process for the removal of MG.

*Keywords:* Sonocatalysis; Fenton process; Chromite; Removal; Cationic dye

### 1. Introduction

Reactive dyes constitute a significant part of colored organic compounds that are widely used in textile industry. Approximately 70% of all textile dyestuffs comprise the azo group ( $-N=N-$ ) in their structure. Due to their high resistance to biodegradation under aerobic conditions, discharging of organic azo dyes into water resources leads to some irreversible detrimental effects on the environment and human health [1–4].

Conventional wastewater treatment processes like coagulation–flocculation, activated sludge, and adsorption mostly result in low decolorization efficiencies for the treatment of textile effluents since these effluents generally include non-biodegradable dye compounds with highly water-soluble large molecules. In addition, there is no degradation of dye molecules in these conventional processes. Instead, pollutants are only transferred to secondary phases, which needs more conditioning [2,5,6]. For that reason, it is

\* Corresponding authors.

essential to find a feasible treatment method for this type of wastewater [7,8].

Advanced oxidation processes (AOPs), which are based on the hydroxyl radical, such as photo-catalysis, sono-catalysis, ozonation, and Fenton processes have attracted special attention in recent years due to their high efficiency and no waste production property [3,5,6,8,9]. The synergistic effects of the many combined AOPs like photo-Fenton, UV/O<sub>3</sub>, UV/H<sub>2</sub>O<sub>2</sub>, and UV/TiO<sub>2</sub> have been currently taken into consideration for increasing efficiency, shortening residence time, and reducing energy need [3,5].

From the various AOPs, the Fenton and ultrasonic irradiation processes have been widely applied for the mineralization of various contaminants from wastewater because of their simplicity and high efficiency. Hydroxyl radical (<sup>•</sup>OH), which is the most influential oxidizing agent in AOPs, can be produced in these processes by the Fenton reaction from mainly ferrous iron based on Eq. (1) or water dissociation due to ultrasonic treatment given in Eq. (2). However, due to its low degradation rate, unassisted ultrasonic irradiation needs more energy, and time with respect to other AOPs. Therefore, it is commonly combined with Fenton process to improve the overall efficiency. On the other hand, homogeneous Fenton process has also certain serious drawbacks, such as necessity of acidic environment (pH 3) for inhibition of the iron precipitation, and recycling and separation of the catalyst after treatment. Thus, utilization of the heterogeneous system, which does not require catalyst separation, performs at milder pH values, and leads to low leached iron, has become a promising practical solution to overcome these obstacles [3,6,8].



A significant body of literature has been recently focused on the use of insoluble iron oxides as a heterogeneous catalyst in Fenton process [1]. So far, various natural and synthesized iron bearing minerals and chemicals such as hematite [1,10], magnetite [9,11,12], goethite [13,14], pyrite [6,8,15], siderite [3], ferrous sulfate heptahydrate [16], ferrihydrite [17], and martite [7] have been used for this purpose. However, the existing literature on chromite is very limited. To the best of our knowledge, there is only one study on refined natural chromite as heterogeneous photo-catalyst conducted by Shaban et al. [18]. In addition, no study has been reported so far on the utilization of natural chromite ore as heterogeneous sono-catalyst. For this reason, a chromite ore was selected, in this study, as a heterogeneous catalyst in the ultrasound-assisted Fenton process for removal of cationic Malachite Green (MG) from aqueous solutions mainly because of its iron content, high availability, and relatively low cost.

## 2. Experimental

### 2.1. Materials

The chromite ore used was obtained from the Kop Chrome Mining Co., (Turkey). The Malachite Green (MG)

dye was supplied from Haining Deer Chemical Co., (China). The other chemicals and reagents used were all analytical grade and purchased from Merck (Germany). Distilled water was used throughout the experiments.

### 2.2. Methods

#### 2.2.1. Preparation of the catalyst

As-received chromite ore was first crushed down to the size range of 0.5–1 cm via jaw and roll crushers. The crushed sample was then subjected to rod milling for obtaining particles with an average size of 30–50 μm. In the last stage, the rod mill product was further ground using a high energy planetary ball mill (LB 200, Turkey) to produce nano-sized chromite particles. The ball to particle mass ratio and the rotation speed used in the planetary ball milling were respective 10:1 and 320 rpm.

#### 2.2.2. Characterization of the catalyst

The major elemental composition was determined with X-ray fluorescence spectrometry. Crystalline phases and microstructural characterizations were determined using X-ray diffraction (XRD) and scanning electron microscopy (SEM) analyses, respectively. The XRD pattern was recorded by a PANalytical Empyrean instrument (Made in Netherlands) over 10°–80° (2°/min) operating with Cu-Kα radiation (λ = 1.54051 Å) at 40 kV, 30 mA, and room temperature. Microstructural investigations were accomplished using high-resolution SEM (HR-SEM). In addition, the associated energy dispersive X-ray measurements (EDX) were done by a Zeiss Sigma 300 instrument furnished with an EDAX analyzer. Fourier transform infrared (FT-IR) spectra of the chromite were recorded by a Tensor 27 Bruker spectrophotometer over 4,000–400 cm<sup>-1</sup> using the KBr pellet technique. The point of zero charge (pH<sub>pzc</sub>) of the chromite was determined with the method suggested by Bessekhouad et al. [19].

Leachability characteristics of the prepared catalyst were also examined at three different pH values in accordance with TS EN 12457–4 standard test [20]. According to this test, a suspension containing deionized water to the catalyst ratio of 10 by weight was first prepared and then continuously agitated with a magnetic stirrer for 24 h at 25°C. The pH values were adjusted with 0.1 M HCl and/or NaOH solutions immediately after preparation of the suspension. After filtration, the solution were analyzed for seven well-known heavy metals using a SensAA Dual atomic absorption spectrometer (AAS).

#### 2.2.3. Heterogeneous sono-Fenton process

In this stage, the prepared nano-sized chromite particles were used as a heterogeneous catalyst in the ultrasound-assisted Fenton process. The ultrasonic treatment parameters were kept constant to focus on the other processing conditions. Therefore, the removal efficiency of MG was studied with varying catalyst dosage (1.0–5.0 g/L), H<sub>2</sub>O<sub>2</sub> concentration (0–50 mM), pH (3–11), and initial dye concentration (10–100 mg/L). The ranges used for the experimental variables were determined based on the preliminary

tests. Batch experiments were performed in 100 mL glass round Erlenmeyer flasks which were put in a Bandelin Sonorex ultrasonic bath (40 kHz, Germany). MG solution used was fixed to 100 mL throughout the experiments. The procedure began with the addition of certain amount of the prepared catalyst into a flask filled with 100 mL MG solution. The predetermined H<sub>2</sub>O<sub>2</sub> was then added into the MG solution to initiate the Fenton reactions. The pH values tested were adjusted with 0.1 M HCl and NaOH solutions, and the measurements were done using a calibrated Mettler Toledo pH meter (China). At the prearranged time intervals, 5 mL sample was withdrawn from the treated solution, and then centrifuged for 5 min at 6,000 rpm by a Hettich EBA 20 Centrifuge, Germany. Finally, MG concentration in the solution was determined with an Optizen pop UV-Vis spectrophotometer (Korea) at 618 nm ( $\lambda_{max}$  for MG). The removal efficiency (RE, %) of MG was calculated by the below equation:

$$RE(\%) = \frac{(A_0 - A_t)}{A_0} \times 100 \quad (3)$$

where  $A_0$  and  $A_t$  show the absorbance values of the solutions before and after the removal process, respectively. In addition, the effects of scavengers, sodium chloride (NaCl), and ethanol (C<sub>2</sub>H<sub>5</sub>OH), on the decolorization of MG were tested for the fixed molar ratio of scavengers to MG as 1:1.

### 3. Results and discussion

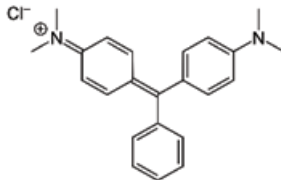
#### 3.1. Characterization results

The main elemental composition of the chromite and the chemical structure of MG are shown in Tables 1 and 2, respectively. As seen from Table 1, the chromite sample

Table 1  
Main elemental composition of the chromite sample

Element	Weight (%)
O	34.53
Mg	12.58
Al	13.43
Si	0.99
Cr	25.8
Fe	12.67

Table 2  
Chemical structure and basic properties of Malachite Green

C.I. name	Chemical formula	Chemical structure	MW (g/mol)	$\lambda_{max}$ (nm)
Malachite Green	C <sub>23</sub> H <sub>25</sub> ClN <sub>2</sub>		364.917	618

mainly includes O, Cr, Mg, Al, Fe, and Si elements as a complex solid solution. Table 2 clearly indicates that MG is a cationic azo dye.

Leachability potentials of Cd, Co, Cr, Cu, Pb, Zn, and Mn elements from the chromite catalyst into the solution were determined at three different pH values, 3, 7.5 (natural), and 11. The obtained concentrations of these heavy metals in the solutions and their toxicity limits according to the regulation of hazardous waste in Turkish standard, storage criteria of solid wastes (Appendix 11-A) [21] are given in Table 3.

As seen in Table 3, higher leaching capacities were obtained in acidic condition as expected and none of the metals except Cd was leached in an extent higher than the toxicity limits for inert waste even at pH 3. In addition, all of the examined metals have leaching capacities far below the toxicity levels for non-hazardous waste. In other words, the chromite sample used as heterogeneous catalyst has no risk for the environment even at the lowest pH value tested.

The XRD patterns of the chromite sample is shown in Fig. 1. As seen from Fig. 1, the sample is mainly composed of chromite mineral. The main diffraction peaks at 2 $\theta$  values of 18.71°, 30.74°, 36.20°, 43.97°, and 58.21° were suited with the literature data [18]. The biggest intensity peak at 2 $\theta$  value of 36.20° can be indexed as the main peak of cubic spinel with face-centered structure [18]. The detected soft peaks were also agreement with chromite sample in the literature studies [22]. The sharp peaks observed prove good crystallinity of the sample, which was made use of the ultrasonic treatment.

Fig. 2 illustrates the FT-IR spectra of the chromite sample. According to this figure, the present absorption bands from 500 to about 600 cm<sup>-1</sup> can be assigned to the stretching vibration of Cr–O for the chromite mineral [23]. In addition, the absorption bands between 500 and 1,000 cm<sup>-1</sup> can be attributed to the bond between groups II and III transition metal cations of spinel oxides and oxygen anion [18,24].

SEM images of the prepared nano-sized chromite particles at different magnifications are given in Fig. 3. As seen from the figure, the prepared sample primarily consists of aggregated microcrystals with particle size ranging from 50 to 1,000 nm. Fig. 3 also shows that the sample surface is uniform.

#### 3.2. Effects of operational parameters

##### 3.2.1. Catalyst dosage

In this stage, a series of experimental runs were conducted to determine the optimum catalyst dosage for

Table 3  
Leachability characteristics of the chromite sample

Element	Leaching test results based on TS EN 12457-4 (ppm)			Toxicity limits for the regulation of hazardous waste in Turkish standard (Appendix 11-A) (mg/L)		
	pH = 3	pH = 7.5 (natural)	pH = 11	IW <sup>a</sup>	NHW <sup>b</sup>	HW <sup>c</sup>
Cd	0.005	0.001	0.003	≤0.004	0.004–0.1	<0.1–0.5
Co	<0.001	<0.001	<0.001	NI <sup>d</sup>	NI <sup>d</sup>	NI <sup>d</sup>
Cr	<0.001	<0.001	<0.001	≤0.05	0.05–1	<1–7
Cu	<0.001	<0.001	<0.001	≤0.2	0.2–5	<5–10
Pb	0.04	0.004	0.02	≤0.05	0.05–1	<1–5
Zn	<0.001	<0.001	<0.001	≤0.4	0.4–5	<5–20
Mn	0.324	0.248	0.125	NI <sup>d</sup>	NI <sup>d</sup>	NI <sup>d</sup>

<sup>a</sup>Inert waste.

<sup>b</sup>Non-hazardous waste.

<sup>c</sup>Hazardous waste.

<sup>d</sup>Not included.

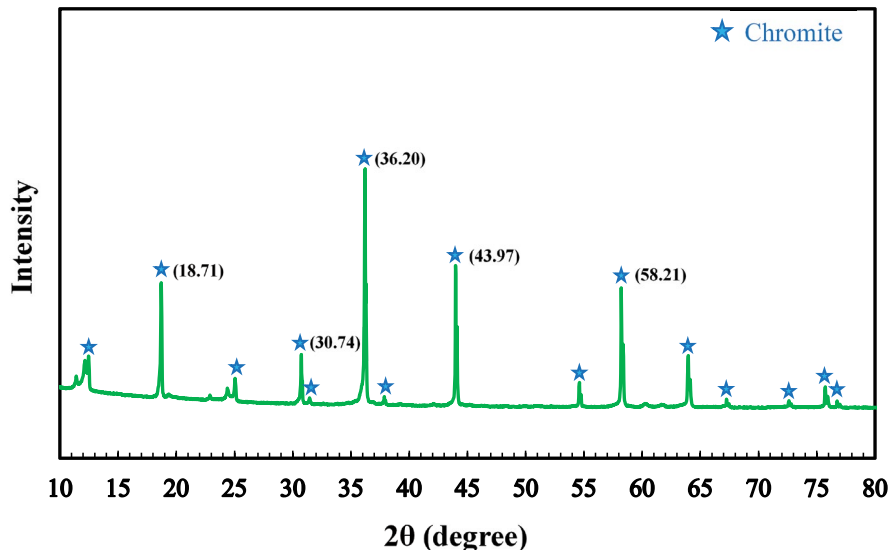


Fig. 1. X-ray powder diffraction pattern of the chromite sample.

removal of MG through ultrasound-assisted heterogeneous Fenton process. In this regard, the catalyst dosages varying from 1 to 5 g/L were tested for the initial MG concentration of 10 mg/L, H<sub>2</sub>O<sub>2</sub> concentration of 30 mM, and natural pH (7.5).

Figs. 4a and b show the effects of catalyst dosage on the removal efficiency of MG as a function of time and for the retention time of 90 min, respectively. As seen from Fig. 4a, the removal efficiency increased with time and the Fenton reactions reached equilibrium at a specified contact time of about 90 min for all of the catalyst dosages tested. Figs. 4a and b together illustrate that the efficiency increased with the increasing dosage up to 3 g/L and then decreased for the higher dosages of 4 and 5 g/L. According to Fig. 4b, for the equilibrium time of 90 min, the degradation efficiency increased from 44.39% to 88.73% for the catalyst dosages of 1 and 3 g/L, respectively. Beyond this point, the efficiency decreased down to 61.61% for the dosage of 5 g/L. As the

highest efficiency values were achieved with 3 g/L for the all tested residence times, this value was selected as the optimum catalyst dosage, and then used to examine the effects of the other operational parameters on the efficiency for the remaining part of this study.

The low efficiency values obtained for the catalyst dosages of 1 and 2 g/L can be attributed to the insufficient formation of Fe<sup>2+</sup> and Cr<sup>2+</sup> ions in the solution, causing less •OH generation and inadequate active sites for the adsorption [25,26]. This can be inferred from Eq. (1) given in the introduction section and Eq. (4), which defines the Fenton reaction involving Cr<sup>2+</sup> ion and can be written as follows:



Conversely, the decreases in the efficiency values from 88.73% to 61.61% are probably resulted from the scavenging

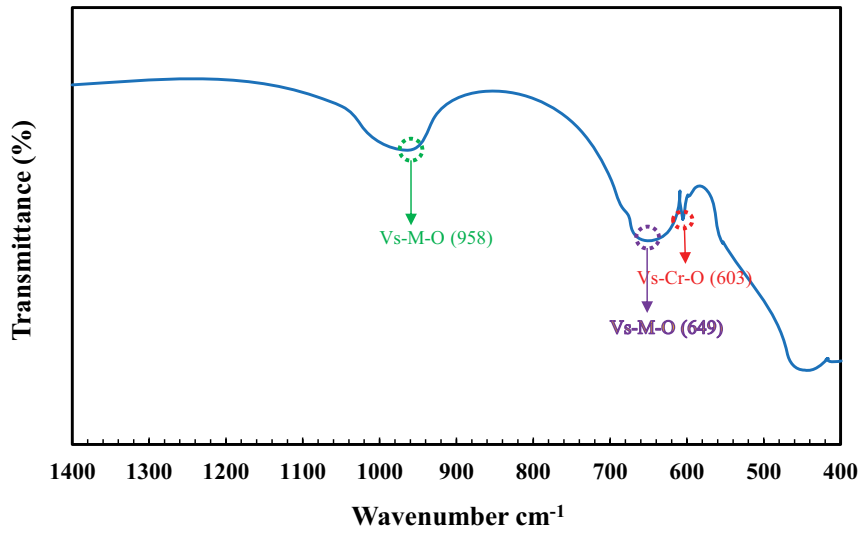


Fig. 2. FT-IR spectra of the chromite.

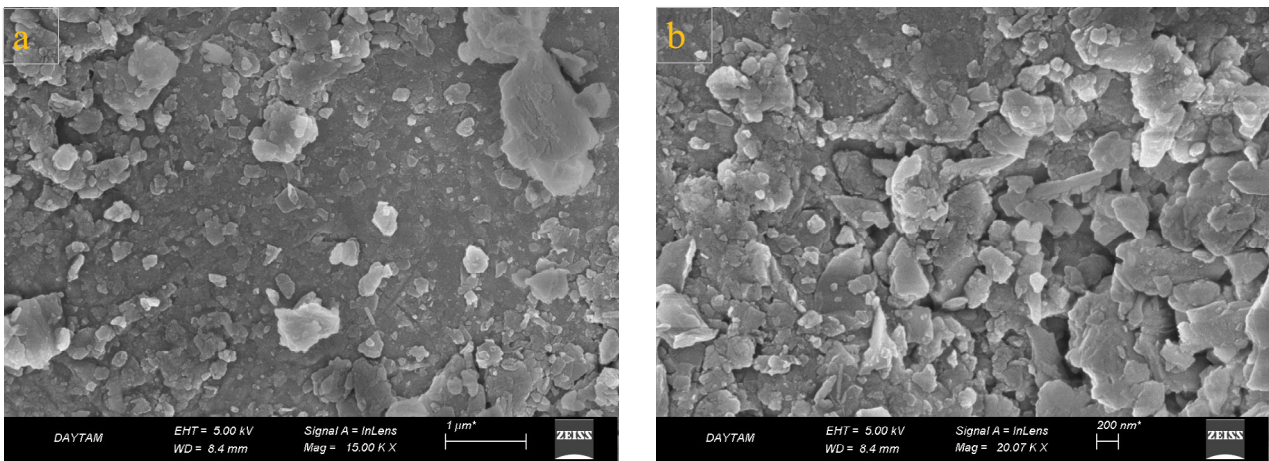


Fig. 3. SEM micrographs of the chromite particles. Scale bar (a) 1 μm and (b) 200 nm.

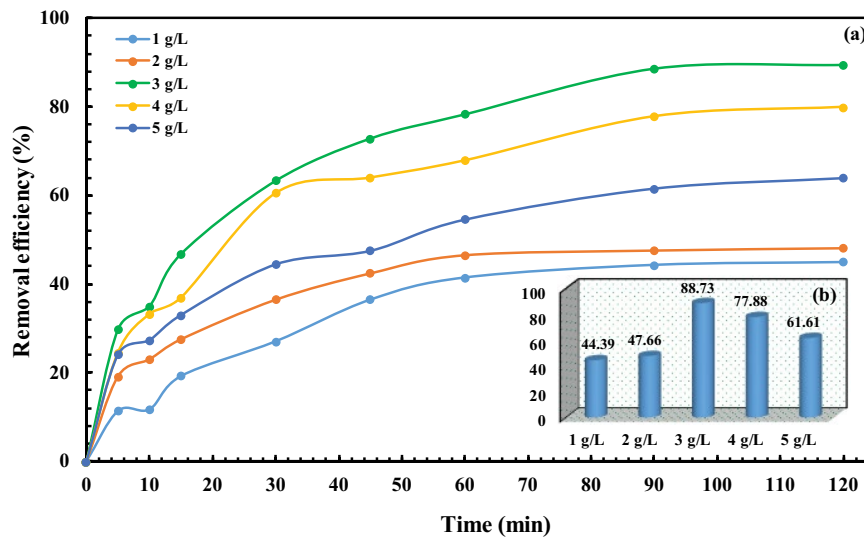
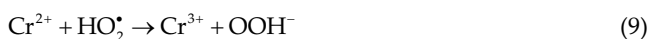


Fig. 4. Effect of catalyst dosage on the removal efficiency (a) as a function of time and (b) for 90 min. Experimental conditions:  $[MG]_0 = 10 \text{ mg/L}$ ,  $[H_2O_2]_0 = 30 \text{ mM}$ , and natural  $\text{pH} = 7.5$ .

effect of  $\text{Fe}^{2+}$  and  $\text{Cr}^{2+}$  ions on the hydroxyl radicals [27,28]. This inference can be expressed as follows:



In addition, high catalyst dosage can cause agglomeration and this limits the formation of hydroxyl and other radicals. This situation is stated in Eqs. (7)–(10). High dosage can also result in the screening effect, preventing ultrasonic waves from creating the cavitation phenomenon essential for the formation of hydroxyl free radicals [3,29].



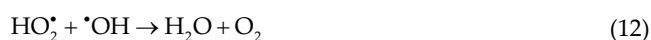
### 3.2.2. Hydrogen peroxide concentration

Hydrogen peroxide ( $\text{H}_2\text{O}_2$ ) has vital importance in the Fenton process so the determination of its optimum concentration can be considered as unavoidable to maximize efficiency. For this purpose, in this set of the experiments,  $\text{H}_2\text{O}_2$  concentrations ranging from 0 to 50 mM were tested to determine its optimum value for the catalyst dosage of 3 g/L found in the previous stage, the initial MG concentration of 10 mg/L and natural pH (7.5). Fig. 5 illustrates the effect of  $\text{H}_2\text{O}_2$  concentration on the removal efficiency of MG as a function of time.

As seen from Fig. 5, for the residence time of 90 min, a very low efficiency value of 26.49% was obtained without

peroxide usage. Fig. 5 also shows that the degradation efficiency increased with  $\text{H}_2\text{O}_2$  concentrations up to 88.74% for 30 mM. However, similar to the previous stage, further increase in peroxide concentrations resulted in a decrease in the efficiency down to 70.53% for 50 mM. Therefore, 30 mM was accepted as the optimum peroxide concentration and used to determine the optimum values for the initial MG concentrations and pH.

The increasing efficiency values for up to peroxide concentration of 30 mM can be attributed to the increasing generation of the hydroxyl radicals [30]. However, the excess amount can react with  $\cdot\text{OH}$ , leading to the formation of  $\text{H}_2\text{O}_2$  and  $\text{O}_2$ . This situation reduces  $\cdot\text{OH}$  concentration in the solution, resulting in a decrease in the degradation efficiency of MG [26,28,31,32]. This inference can be expressed as follows:



### 3.2.3. Initial dye concentration

In this stage, initial MG concentrations varying from 10 to 100 mg/L were tested at natural pH for the catalyst dosage of 3 g/L and peroxide concentration of 30 mM, which were determined as the optimum values in the previous stages. Fig. 6 displays the effect of initial MG concentration on the degradation efficiency as a function of time.

According to Fig. 6, the efficiency substantially decreased with increasing MG concentrations. For the reaction time of 90 min, the efficiency reduced from 88.74% for the initial MG concentration of 10 mg/L down to 54.46% for the highest tested concentration of 100 mg/L.

In this experimental set, the decreasing efficiency values with the increasing MG concentrations can be resulted from the insufficient generation of hydroxyl radical and

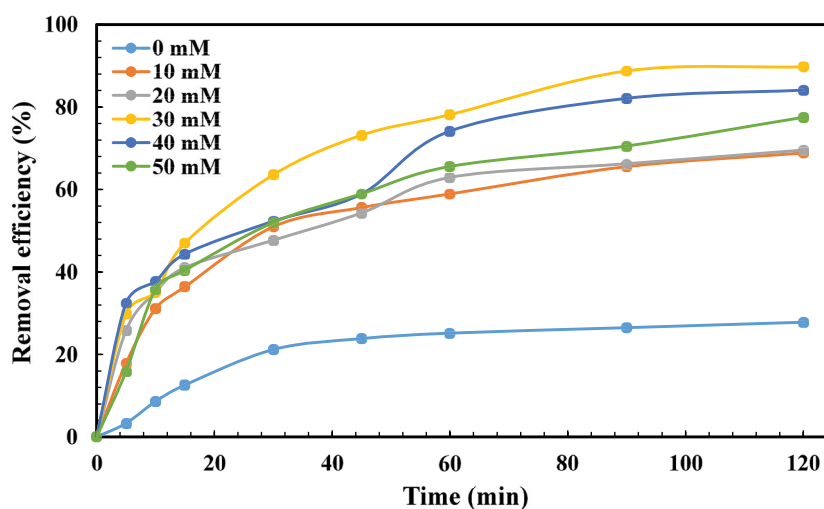


Fig. 5. Effect of  $\text{H}_2\text{O}_2$  concentration on the degradation efficiency of MG. Experimental conditions: Catalyst dosage = 3.0 g/L,  $[\text{MG}]_0 = 10$  mg/L, and natural pH = 7.5.

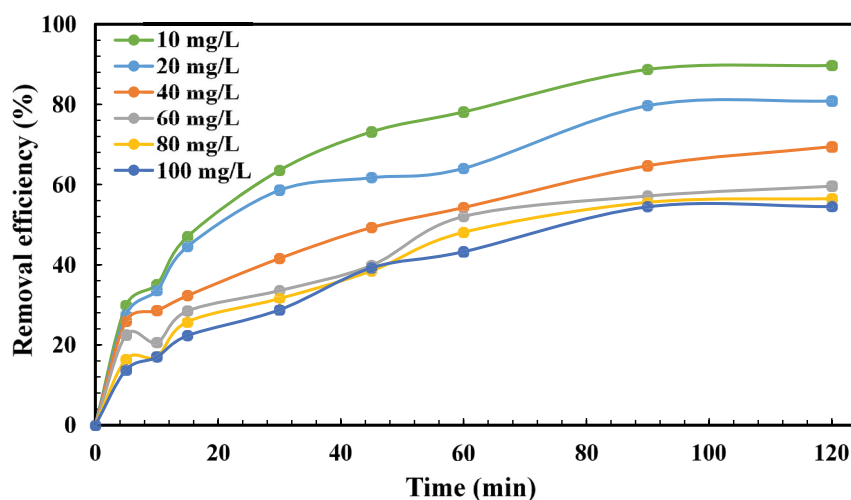


Fig. 6. Effect of initial dye concentration on the decolorization efficiency. Experimental conditions: Catalyst dosage = 3 g/L,  $[H_2O_2]_0 = 30$  mM, and natural pH = 7.5.

inadequate active sites for the adsorption because of the fixed catalyst dosage and peroxide concentration, and constant ultrasonic power used [33,34]. In addition, as far as is known, adsorption occurs firstly, and then it is followed by degradation in heterogeneous Fenton process. With increasing dye concentrations, the availability of surface active sites begins to decrease due to adsorption of increasing number of dye molecules. After a point, there is no active sites on catalyst surface essential for adsorption. This situation can diminish the hydroxyl radicals' production, leading to a reduction in efficiency. Another possible mechanism for the decreasing efficiency can be resulted from the screening of dye molecules which hinders ultrasonic waves from passing through the solution. This effect decreases the turbulence and the cavitation phenomena, causing reduced mass transfer and  $\cdot OH$  formation [6]. Lastly, the catalyst particles which adsorb dye molecules in high amounts begin to lose their adsorption ability. This situation can also result in less  $\cdot OH$  generation [35].

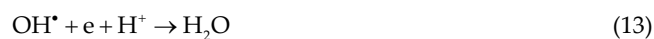
#### 3.2.4. Effect of pH

Initial pH is a very important parameter since it determines the route of the Fenton processes. In this set of experiments, pH values ranging from 3 to 11 were tested to determine its optimum value for the catalyst dosage of 3 g/L, peroxide concentration of 30 mM, and MG concentration of 100 mg/L. Fig. 7 illustrates the effect of initial pH on the removal efficiency of MG as a function of time.

As seen from this figure, the efficiency increased dramatically with increasing pH. From the experimental results, for the reaction time of 120 min, the removal efficiency of MG was obtained 88.22% for pH 11 and 35.07% for pH 3.

Fig. 8 exhibits the  $pH_{pzc}$  plot of the chromite sample. According to this figure, the  $pH_{pzc}$  value was determined as 7.65, indicating that the chromite surface is positively charged for the pH values below 7.65 and negatively charged above this point.

As seen from Figs. 7 and 8, for pH values lower than 8.0, as the chromite catalyst surface charge is positively charged, electrostatic repulsion takes place between the catalyst surface and the cationic MG dye, which will result in a reduction in adsorption efficiency [36]. In addition, the low removal efficiency of MG at pH value of 3.0 may be attributed to the scavenging effect of hydrogen ions at this strongly acidic condition, which is expressed as follows [37]:



In contrast, a significant increase in the adsorption of cationic MG was observed due to the negative surface of the catalyst at high pH. For example, the increase in degradation efficiency at pH 11 can be attributed to the enhancement in adsorption of cationic MG dye molecules by the combination of electrostatic interactions and hydrogen bonding through the strongest interaction. Similar results have also been reported by Öztürk to Malkoc [38]. Moreover, the increment of adsorption capacity at pH higher than 9.0 would probably be due to the alkaline fading of MG in which the dye turns into a carbinol base at these pH values [39].

#### 3.3. Effect of scavenging compounds

The effects of inorganic salts and organic compounds on the decolorization of MG solution were also tested. For this purpose, sodium chloride (NaCl) and ethanol ( $C_2H_5OH$ ) were used with a fixed concentration of 0.01 M. In this stage, the adsorption tests were performed at the natural pH for the catalyst dosage of 3 g/L, peroxide concentration of 30 mM, and MG concentration of 10 mg/L. Fig. 9 presents the effects of scavengers on the decolorization efficiency of MG. According to Fig. 9, for the reaction time of 120 min, the efficiency of 89.74% dropped down to 64.81% and 40.45% for the addition of NaCl and  $C_2H_5OH$ , respectively.

Chloride is a common anion in the textile wastewaters, which acts as a scavenger for the hydroxyl radicals. In this

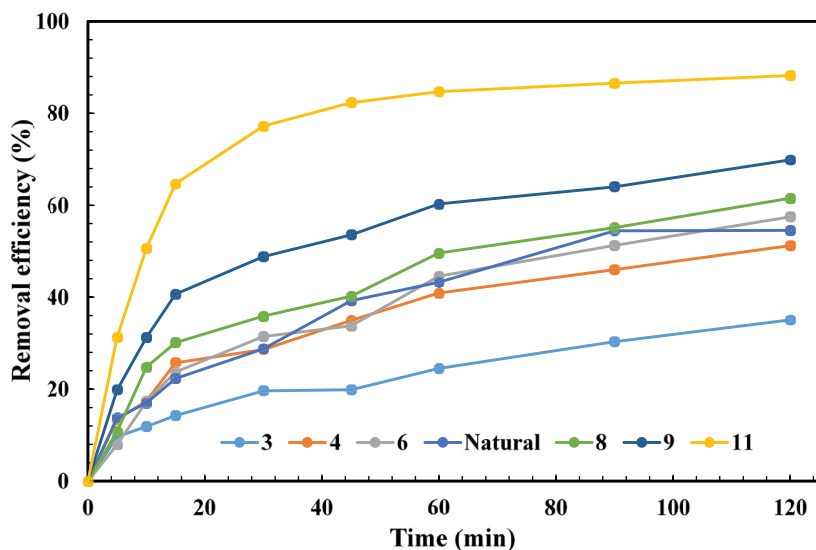


Fig. 7. Effect of initial pH on the degradation efficiency of MG. Experimental conditions: Catalyst dosage = 3 g/L,  $[H_2O_2]_0 = 30$  mM, and  $[MG]_0 = 100$  mg/L.

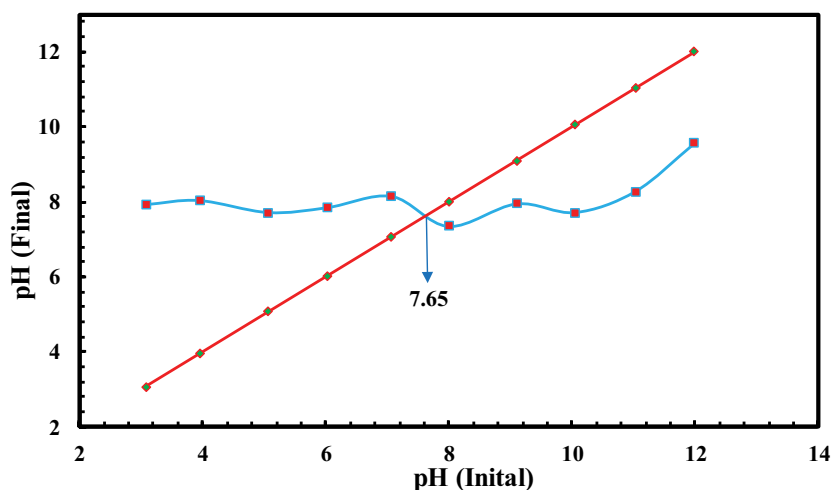


Fig. 8.  $pH_{pzc}$  plot of the chromite sample.

study, as seen from Fig. 9, the inhibitory effect of chloride is relatively low since it reacts with  $\cdot OH$  and generates radical species with lower oxidation powers as shown in the below equation. The decrease in the degradation efficiency can also be due to the occupation of active superficial sites by chloride anion, which limits the Fenton reactions [3,7].



On the other hand, Fig. 9 points out that the addition of ethanol caused a substantial reduction in the efficiency which has been indicated by a number of researchers in various AOPs [3,7,40,41] and can be expressed as follows:



#### 3.4. Comparison of various treatment processes

The effects of various treatment processes on the degradation efficiency of MG were also examined. Within this scope, in this stage, a number of the experimental set were designed using ultrasonic (US), peroxide, catalytic, and various combinations of these processes. The adsorption tests were performed at natural pH for the catalyst dosage of 3 g/L, peroxide concentration of 30 mM, and MG concentration of 10 mg/L. Fig. 10 displays the effects of these treatment processes for the reaction time of 90 min.

As seen from Fig. 10, the effects of ultrasound, peroxide, and a combination of these on the decolorization of MG solution were insignificant as expected. The degradation efficiencies of the aforementioned processes were lower than 15% where ultrasound alone provided the lowest value of 5.29%. According to the literature, ultrasonic treatment



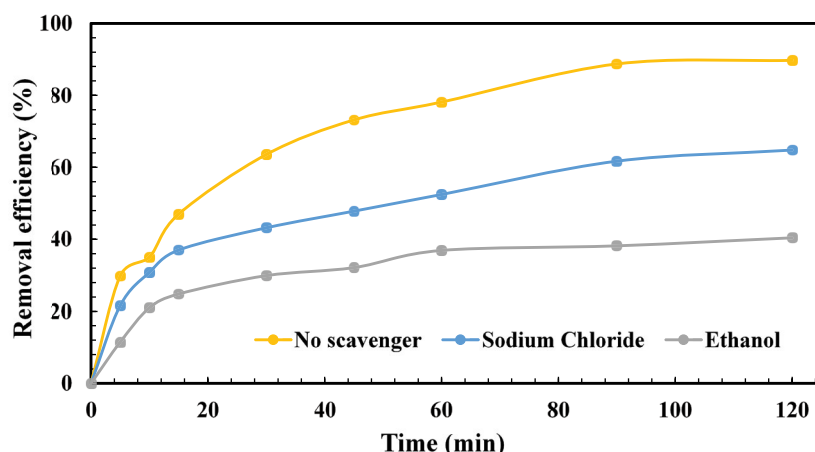


Fig. 9. Effect of scavengers on the decolorization efficiency of MG. Experimental conditions: Catalyst dosage = 3 g/L,  $[H_2O_2]_0 = 30$  mM,  $[MG]_0 = 10$  mg/L, natural pH = 7.5, and  $[NaCl] = [C_2H_5OH] = 0.01$  M.

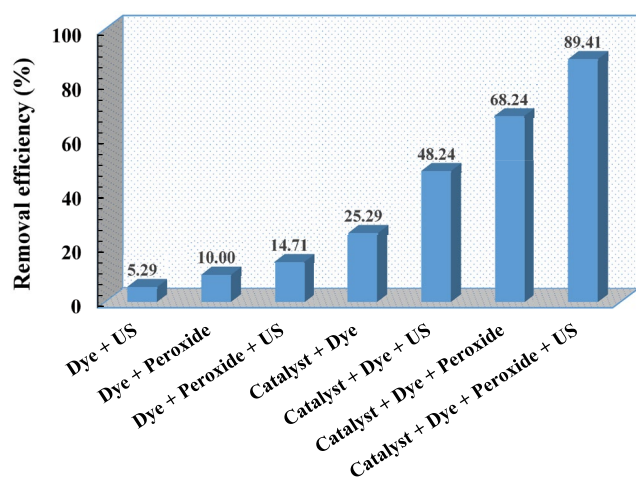


Fig. 10. Effects of various treatment processes on the removal efficiency of MG for the reaction time of 90 min. Experimental conditions: Catalyst dosage = 3 g/L,  $[H_2O_2]_0 = 30$  mM,  $[MG]_0 = 10$  mg/L, and natural pH = 7.5.

has very low efficiency for the degradation of organic compounds, and it needs a very long time and high energy for complete degradation. Ultrasonic degradation process can be enhanced with peroxide usage owing to the generation of hydroxyl radicals based on the Eq. (16) [3]. This is also valid for this study in which the efficiency increased with the addition of peroxide up to 14.71%.



In the absence of ultrasound and peroxide, the efficiency of 25.29% was obtained with the catalyst alone (adsorption). This dye removal is resulted from the physical adsorption because Fenton reactions do not occur in the absence of ultrasound and peroxide. The efficiency values increased to 48.24% and 68.24% with the addition of ultrasound and peroxide to the catalyst only treatment, respectively. This can be explained by increasing number of oxidizing

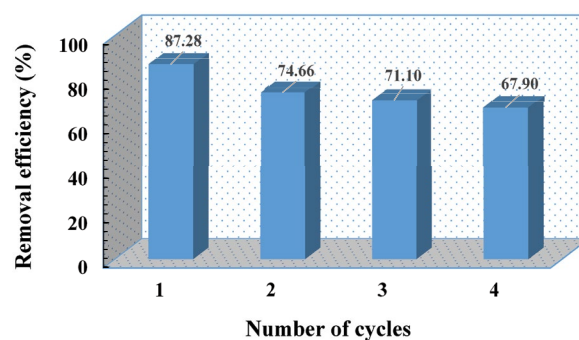


Fig. 11. Reusability of the catalyst within four consecutive experimental runs. Experimental conditions: Catalyst dosage = 3 g/L,  $[H_2O_2]_0 = 30$  mM,  $[MG]_0 = 10$  mg/L, and natural pH = 7.5.

agents in the solution with ultrasonic treatment and peroxide usage, contributing to the degradation of the dye. The best result, 89.41%, was achieved with the synergistic effect of ultrasound and peroxide on the catalyst surface, confirming the suitable catalytic properties of the natural chromite for Fenton process. The possible mechanism behind this can be the dispersive effect of ultrasonic irradiation on the catalyst. In other words, ultrasonic treatment inhibits the aggregation of catalyst nanoparticles, providing more available active sites for Fenton reactions. In addition, tensile strength between solid and liquid phase can be reduced by ultrasonic irradiation, enhancing the catalytic Fenton reaction [3]. Consequently, the combination of ultrasonic irradiation and Fenton process results in more oxidizing agents and accordingly improved the degradation rate of the target pollutant.

### 3.5. Reusability of the catalyst

From a practical point of view, one of the most important properties of a catalyst is its long-term reusability. Therefore, reusability of the catalyst were also examined by four consecutive cycles. The operational parameters were kept the same with the previous stage. After each cycle, the

Table 4  
Intermediates produced during the degradation of MG

No.	Compound	Retention time (min)	Main fragment (m/z)	Molecular structure
1	p,p'-Benzylidenebis (N,N dimethylaniline)	34.720	253 (100%) 330 (72.2%) 165 (41.3%) 209 (23.8%) 210 (23.7%)	
2	2,2,4-trimethyl-3-((3E,7E,11E)-3,8,12,16-tetramethylheptadeca-3,7,11,15-tetraen-1-yl)cyclohexanol	33.576	69 (100%) 81 (54.0%) 41 (34.3%) 55 (21.1%) 95 (18.9%) 148 (100%)	
3	Methanone, 4-(dimethylamino)phenyl] phenyl	24.180	225 (61.0%) 77 (32.3%) 105 (16.0%) 224 (11.7%) 73 (100%)	
4	5-hydroxy-6,7,8-trimethoxy-2,3-dimethyl-4H-chromen-4-one	15.794	265 (48.5%) 75 (34.2%) 307 (32.2%) 57 (31.7%)	
5	2,3,4-Trimethoxyacetophenone	15.206	193 (100%) 43 (55.8%) 167 (55.3%) 57 (49.9%) 41 (35.6%)	
6	5,6,6-trimethyl-5-(3-oxobut-1-en-1-yl)-1-oxaspiro[2.5]octan-4-one	14.678	193 (100%) 97 (97.1%) 57 (79.5%) 43 (65.7%) 41 (50.6%)	
7	1-(2,6,6 trimethylcyclohex-1-en-1-yl) ethanol	13.130	168 (100%) 57 (91.9%) 43 (77.0%) 91 (69.9%) 153 (66.9%)	
8	Pyrimido [1,2-α] azepine, 2,3,4,6,7,8,9,10-octahydropyrimido	11.270	151 (100%) 152 (88.6%) 123 (70.1%) 96 (62.5%) 41 (57.6%)	

used catalyst was separated from the solution, washed with distilled water and dried for the next run.

The removal efficiencies obtained for these four successive tests are demonstrated in Fig. 11. As seen from this figure, the efficiency reduced from 87.28% to 67.90% after four consecutive cycles, corresponding to only 22.20% decline in efficiency. This result points out the reusability of the chromite particles as a catalyst.

### 3.6. Determination of intermediate products

Intermediate products formed during the degradation of MG were determined via GC–MS analysis to monitor the progress in the decomposition of the target pollutant through the heterogeneous sono-Fenton process used. Table 4 exhibits the intermediates produced during the degradation of MG.

As seen in Table 4, prior to the completely decomposed to water and carbon dioxide, MG transformed into the intermediates such as p,p'-benzylidenebis, pyrimido [1,2- $\alpha$ ] azepine, 1-(2,6,6 trimethylcyclohex-1-en-1-yl) ethanol, methanone, 2,3,4-trimethoxyacetophenone, 5-hydroxy-6,7,8-trimethoxy-2,3-dimethyl-4H-chromen-4-one, 2,2,4-trimethyl-3-((3E,7E,11E)-3,8,12,16-tetramethyl heptadeca-3,7,11,15-tetraen-1-yl) cyclohexanol, and 5,6,6-trimethyl-5-(3-oxobut-1-en-1-yl)-1-oxaspiro [2.5] octan-4-one throughout the degradation process. The observed transformation of the structures from complex to simple forms confirmed the high degradation efficiency of MG through the sono-Fenton process over chromite nanoparticles [3].

## 4. Conclusion

In this study, the utilization potential of the prepared chromite nanoparticles as a catalyst in the heterogeneous sono-Fenton process was examined for the removal of MG from aqueous solutions. According to the experimental results, the efficiency increased with the catalyst dosage and peroxide concentration up to a point while it decreased gradually with initial dye concentration. Specifically, the optimum efficiency, 89%, was attained for 3 g/L catalyst dosage, 30 mM peroxide concentration, and 10 mg/L MG concentration at natural pH (7.5) for 90 min. However, excessive amounts of the catalyst and peroxide caused reductions in the efficiency down to 61.61% and 70.53% for the respective 5 g/L and 50 mM. The best overall efficiency was obtained for the combined effect of ultrasound and peroxide on the catalyst surface. In addition, from the reusability tests, only 22.20% reduction in the efficiency were observed after four consecutive cycles. On the other hand, the efficiency substantially reduced down to 40.45% in the presence of ethanol. AAS analysis proved that the catalyst has no risk for the environment even at the lowest pH value tested. GC–MS analysis confirmed the high degradation efficiency of MG. In conclusion, all of these tests and analyses suggested that natural ground chromite mineral can be easily and effectively used as a catalyst in the ultrasound-assisted heterogeneous Fenton process. The most significant advantage of the process is the applicability at mild pH values, providing less operational cost. However, the catalyst dosage and peroxide concentration must be carefully controlled for maximum efficiency.

## Acknowledgment

Atatürk University Scientific Research Council financially supports this study in the context of a project (Project No: FHD-2018-688), and also the technical support by East Anatolia High Technology Application and Research Center (DAYTAM) from Atatürk University is thankfully appreciated.

## References

- [1] F. Araujo, L. Yokoyama, L. Teixeira, J. Campos, Heterogeneous Fenton process using the mineral hematite for the discoloration of a reactive dye solution, *Braz. J. Chem. Eng.*, 28 (2011) 605–616.
- [2] Z. Eren, Ultrasound as a basic and auxiliary process for dye remediation: a review, *J. Environ. Manage.*, 104 (2012) 127–141.
- [3] O. Acisli, A. Khataee, R. Darvishi Cheshmeh Soltani, S. Karaca, Ultrasound-assisted Fenton process using siderite nanoparticles prepared via planetary ball milling for removal of reactive yellow 81 in aqueous phase, *Ultrason. Sonochem.*, 35 (2017) 210–218.
- [4] A. Hassani, R. Darvishi Cheshmeh Soltani, M. Kiranşan, S. Karaca, C. Karaca, A. Khataee, Ultrasound-assisted adsorption of textile dyes using modified nanoclay: central composite design optimization, *Korean J. Chem. Eng.*, 33 (2016) 178–188.
- [5] J.M. Monteagudo, A. Durán, I.S. Martín, S. García, Ultrasound-assisted homogeneous photocatalytic degradation of Reactive Blue 4 in aqueous solution, *Appl. Catal., B*, 152–153 (2014) 59–67.
- [6] A. Khataee, P. Gholami, B. Vahid, S.W. Joo, Heterogeneous sono-Fenton process using pyrite nanorods prepared by non-thermal plasma for degradation of an anthraquinone dye, *Ultrason. Sonochem.*, 32 (2016) 357–370.
- [7] M. Dindarsafa, A. Khataee, B. Kaymak, B. Vahid, A. Karimi, A. Rahmani, Heterogeneous sono-Fenton-like process using martite nanocatalyst prepared by high energy planetary ball milling for treatment of a textile dye, *Ultrason. Sonochem.*, 34 (2017) 389–399.
- [8] A. Khataee, A. Karimi, S. Arefi-Oskoui, R.D.C. Soltani, Y. Hanifehpour, B. Soltani, S.W. Joo, Sonochemical synthesis of Pr-doped ZnO nanoparticles for sonocatalytic degradation of Acid Red 17, *Ultrason. Sonochem.*, 22 (2015) 371–381.
- [9] L. Hou, L. Wang, S. Royer, H. Zhang, Ultrasound-assisted heterogeneous Fenton-like degradation of tetracycline over a magnetite catalyst, *J. Hazard. Mater.*, 302 (2016) 458–467.
- [10] L. Demarchis, M. Minella, R. Nisticò, V. Maurino, C. Minero, D. Vione, Photo-Fenton reaction in the presence of morphologically controlled hematite as iron source, *J. Photochem. Photobiol., A*, 307–308 (2015) 99–107.
- [11] R. Huang, Z. Fang, X. Fang, E.P. Tsang, Ultrasonic Fenton-like catalytic degradation of bisphenol A by ferrous oxide ( $\text{Fe}_3\text{O}_4$ ) nanoparticles prepared from steel pickling waste liquor, *J. Colloid Interface Sci.*, 436 (2014) 258–266.
- [12] X. Liang, Y. Zhong, H. He, P. Yuan, J. Zhu, S. Zhu, Z. Jiang, The application of chromium substituted magnetite as heterogeneous Fenton catalyst for the degradation of aqueous cationic and anionic dyes, *Chem. Eng. J.*, 191 (2012) 177–184.
- [13] A.M. Mesquita, I.R. Guimarães, G.M.M.d. Castro, M.A. Gonçalves, T.C. Ramalho, M.C. Guerreiro, Boron as a promoter in the goethite ( $\alpha\text{-FeOOH}$ ) phase: organic compound degradation by Fenton reaction, *Appl. Catal., B*, 192 (2016) 286–295.
- [14] Z.-R. Lin, L. Zhao, Y.-H. Dong, Quantitative characterization of hydroxyl radical generation in a goethite-catalyzed Fenton-like reaction, *Chemosphere*, 141 (2015) 7–12.
- [15] W. Wang, Y. Qu, B. Yang, X. Liu, W. Su, Lactate oxidation in pyrite suspension: a Fenton-like process in situ generating  $\text{H}_2\text{O}_2$ , *Chemosphere*, 86 (2012) 376–382.
- [16] H.B. Ammar, Sono-Fenton process for metronidazole degradation in aqueous solution: effect of acoustic cavitation and peroxydisulfate anion, *Ultrason. Sonochem.*, 33 (2016) 164–169.

- [17] W.P. Kwan, B.M. Voelker, Decomposition of hydrogen peroxide and organic compounds in the presence of dissolved iron and ferrihydrite, *Environ. Sci. Technol.*, 36 (2002) 1467–1476.
- [18] M. Shaban, M.R. Abukhadra, S.S. Ibrahim, M.G. Shahien, Photocatalytic degradation and photo-Fenton oxidation of Congo red dye pollutants in water using natural chromite—response surface optimization, *Appl. Water Sci.*, 7 (2017) 4743–4756.
- [19] Y. Bessekhouad, D. Robert, J.V. Weber, N. Chaoui, Effect of alkaline-doped TiO<sub>2</sub> on photocatalytic efficiency, *J. Photochem. Photobiol., A*, 167 (2004) 49–57.
- [20] T.S.I. TS EN 12457–4, Part 4. One Stage Batch Test at a Liquid to Solid Ratio of 10 L/kg for Materials with Particle Size Below 10 mm (Without or with Size Reduction), Characterization of Waste-Leaching-Compliance Test for Leaching of Granular Waste Materials and Sludge, Turkish Legislation for Standardization, Turkey, 2004.
- [21] T.S. Institute, Appendix 11-A: Storage Criteria of Solid Wastes, The Regulation of Hazardous Waste in Turkish Standard, Turkey, 2005.
- [22] M.H. Morcali, C. Eyuboglu, S. Aktas, Synthesis of nanosized Cr<sub>2</sub>O<sub>3</sub> from turkish chromite concentrates with sodium borohydride (NaBH<sub>4</sub>) as reducing agent, *Int. J. Miner. Process.*, 157 (2016) 7–15.
- [23] S.K. Durrani, S.Z. Hussain, K. Saeed, Y. Khan, M. Arif, N. Ahmed, Hydrothermal synthesis and characterization of nanosized transition metal chromite spinels, *Turk. J. Chem.*, 36 (2012) 111–120.
- [24] T. Moroz, L. Razvorotneva, T. Grigorieva, M. Mazurov, D. Arkhipenko, V. Prugov, Formation of spinel from hydro-talcite-like minerals and destruction of chromite implanted by inorganic salts, *Appl. Clay Sci.*, 18 (2001) 29–36.
- [25] X. Hu, B. Liu, Y. Deng, H. Chen, S. Luo, C. Sun, P. Yang, S. Yang, Adsorption and heterogeneous Fenton degradation of 17 $\alpha$ -methyltestosterone on nano Fe<sub>3</sub>O<sub>4</sub>/MWCNTs in aqueous solution, *Appl. Catal., B*, 107 (2011) 274–283.
- [26] L. Xu, J. Wang, Fenton-like degradation of 2,4-dichlorophenol using Fe<sub>3</sub>O<sub>4</sub> magnetic nanoparticles, *Appl. Catal., B*, 123–124 (2012) 117–126.
- [27] Y. Kuang, Q. Wang, Z. Chen, M. Megharaj, R. Naidu, Heterogeneous Fenton-like oxidation of monochlorobenzene using green synthesis of iron nanoparticles, *J. Colloid Interface Sci.*, 410 (2013) 67–73.
- [28] O. Acisli, A. Khataee, S. Karaca, A. Karimi, E. Dogan, Combination of ultrasonic and Fenton processes in the presence of magnetite nanostructures prepared by high energy planetary ball mill, *Ultrason. Sonochem.*, 34 (2017) 754–762.
- [29] A. Khataee, T.S. Rad, B. Vahid, S. Khorram, Preparation of zeolite nanorods by corona discharge plasma for degradation of phenazopyridine by heterogeneous sono-Fenton-like process, *Ultrason. Sonochem.*, 33 (2016) 37–46.
- [30] M. Sheydaei, S. Aber, A. Khataee, Degradation of amoxicillin in aqueous solution using nanolepidocrocite chips/H<sub>2</sub>O<sub>2</sub>/UV: optimization and kinetics studies, *J. Ind. Eng. Chem.*, 20 (2014) 1772–1778.
- [31] S. Bae, D. Kim, W. Lee, Degradation of diclofenac by pyrite catalyzed Fenton oxidation, *Appl. Catal., B*, 134 (2013) 93–102.
- [32] T. Xu, Y. Liu, F. Ge, L. Liu, Y. Ouyang, Application of response surface methodology for optimization of azocarmine B removal by heterogeneous photo-Fenton process using hydroxy-iron–aluminum pillared bentonite, *Appl. Surf. Sci.*, 280 (2013) 926–932.
- [33] M. Neamtu, C. Zaharia, C. Catrinescu, A. Yediler, M. Macoveanu, A. Kettrup, Fe-exchanged Y zeolite as catalyst for wet peroxide oxidation of reactive azo dye procion marine H-EXL, *Appl. Catal., B*, 48 (2004) 287–294.
- [34] A. Khataee, R.D.C. Soltani, A. Karimi, S.W. Joo, Sonocatalytic degradation of a textile dye over Gd-doped ZnO nanoparticles synthesized through sonochemical process, *Ultrason. Sonochem.*, 23 (2015) 219–230.
- [35] A. Hassani, G. Çelikdağ, P. Eghbali, M. Sevim, S. Karaca, Ö. Metin, Heterogeneous sono-Fenton-like process using magnetic cobalt ferrite-reduced graphene oxide (CoFe<sub>2</sub>O<sub>4</sub>-rGO) nanocomposite for the removal of organic dyes from aqueous solution, *Ultrason. Sonochem.*, 40 (2018) 841–852.
- [36] O. Acisli, A. Khataee, S. Karaca, M. Sheydaei, Modification of nanosized natural montmorillonite for ultrasound-enhanced adsorption of Acid Red 17, *Ultrason. Sonochem.*, 31 (2016) 116–121.
- [37] H. Zhang, J. Zhang, C. Zhang, F. Liu, D. Zhang, Degradation of CI Acid Orange 7 by the advanced Fenton process in combination with ultrasonic irradiation, *Ultrason. Sonochem.*, 16 (2009) 325–330.
- [38] A. Öztürk, E. Malkoc, Adsorptive potential of cationic Basic Yellow 2 (BY2) dye onto natural untreated clay (NUC) from aqueous phase: mass transfer analysis, kinetic and equilibrium profile, *Appl. Surf. Sci.*, 299 (2014) 105–115.
- [39] L. Leng, X. Yuan, G. Zeng, J. Shao, X. Chen, Z. Wu, H. Wang, X. Peng, Surface characterization of rice husk bio-char produced by liquefaction and application for cationic dye (Malachite green) adsorption, *Fuel*, 155 (2015) 77–85.
- [40] H. Wang, X. Yuan, Y. Wu, G. Zeng, X. Chen, L. Leng, Z. Wu, L. Jiang, H. Li, Facile synthesis of amino-functionalized titanium metal-organic frameworks and their superior visible-light photocatalytic activity for Cr(VI) reduction, *J. Hazard. Mater.*, 286 (2015) 187–194.
- [41] M. Zhou, H. Yang, T. Xian, R.S. Li, H.M. Zhang, X.X. Wang, Sonocatalytic degradation of RhB over LuFeO<sub>3</sub> particles under ultrasonic irradiation, *J. Hazard. Mater.*, 289 (2015) 149–157.